THESIS

THROUGHPUT-NORMALIZED METHANE EMISSION THRESHOLDS FOR DIAGNOSING ROD PACKING SEAL FAILURE IN RECIPROCATING COMPRESSORS

Submitted by

Ethan Rimelman

Department of Systems Engineering

In partial fulfillment of the requirements

For the Degree of Master of Science

Colorado State University

Fort Collins, Colorado

Summer 2026

Master's Committee:

Advisor: Anna Lily Hodshire

Kira Shonkwiler
Daniel B. Olsen

ABSTRACT

THROUGHPUT-NORMALIZED METHANE EMISSION THRESHOLDS FOR DIAGNOSING ROD PACKING SEAL FAILURE IN RECIPROCATING COMPRESSORS

Reducing the atmospheric concentration of greenhouse gases demands accurate quantification of methane sources. Compressors in the oil and gas industry generate significant emissions that often depend on the condition of the equipment. Estimating leak sources across different operational states provides a basis for assessing maintenance urgency.

Traditional emission factors assign a single rate regardless of compressor size, but emission magnitudes are not necessarily proportional to the amount of gas a given unit processes. Using a throughput normalized approach captures the dependency of emissions from reciprocating compressors with their rated power. Using data from Zimmerle et al.'s Gathering Emission Factor (GEF) field study of gathering and boosting stations, it is shown that compressors below 1000 HP exhibit a median rod packing fractional loss approximately 3.6 times that of larger units, with a larger difference of roughly 57 times for blowdown vent emissions. These differences show that smaller compressors lose a greater fraction of throughput across both emission sources.

Applying a log-log linear fit to the GEF data, a framework is established for assessing and diagnosing rod packing seal failure. Within this model, the fractional-loss threshold indicating likely seal failure (95th percentile) is approximately 0.23% for a 350 HP unit, representative of a production-scale vapor recovery compressor, and 0.044% for a 1000 HP unit.

A model for estimating throughput normalized emissions is valuable for modeling and regulatory functions. For mitigating emissions, policy could adopt a framework that assigns maintenance actions dynamically, with thresholds based on associated engine power.

TABLE OF CONTENTS

LIST OF TABLES

LIST OF FIGURES

1 INTRODUCTION

Natural gas has accounted for about 38% of U.S. total energy production in 2024 and has been the largest source of U.S. domestic energy production every year since 2011 [U.S. Energy Information Administration, 2024]. Methane typically comprises 70–90% of natural gas by volume [U.S. Energy Information Administration, 2023] and is a potent but short-lived greenhouse gas (GHG), with a global warming potential (GWP) of 81–83 over 20 years, and 27–30 over 100 years [Forster et al., 2021, U.S. Environmental Protection Agency, 2024e]. Both the high warming potential and short atmospheric lifespan make methane emissions reduction a powerful lever for achieving short term climate goals, but accurately estimating emission sources is a precondition for reducing total releases.

A persistent challenge in methane quantification is the reconciliation of top-down and bottom-up inventories [Brandt et al., 2014, Alvarez et al., 2018]. Top-down accounting for methane entails measurement of many aggregated sources, such as a single satellite capture of an entire region's emissions. Bottom up inventories differ in that they compile measured sources and their frequency to generate an aggregate prediction. Many studies at the regional level have encountered significant discrepancies between top-down and bottom-up methods [Brandt et al., 2014, Zavala-Araiza et al., 2015, Alvarez et al., 2018]. Through top-down measurements, it is estimated that oil and natural gas systems were responsible for 72–97 Tg of methane released into the atmosphere, comprising approximately 23% of anthropogenic methane [Jackson et al., 2020, Saunois et al., 2020]. Bottom-up facility-scale assessments estimate that 2.3% of gross U.S. natural gas production is lost to the atmosphere across the supply chain, equivalent to 13 $\pm$ 2 Tg CH_4 per year [Alvarez et al., 2018]. This leak rate approaches the 2.7% [Alvarez et al., 2018] to 3.2% [Alvarez et al., 2012] threshold at which the climate benefit of substituting natural gas for coal is entirely offset, highlighting the urgency of identifying and reducing emission sources throughout the gas supply chain.

Oil and gas systems are typically divided by sector. The upstream sector includes all pre-production and production activities, which include drilling, extraction, well stimulation, and early processing on the wellpad. Midstream describes the transport and intermediate handling of produced fluids, including gathering systems, booster and compressor stations, and transmission pipelines that maintain flow and pressure as gas moves from the field to processing or storage. Downstream, or distribution, covers the provision and delivery of piped oil and gas to end users.

Compressor stations emit approximately 43% of total methane released across the U.S. natural gas supply chain and are the single largest source category at processing, transmission, and storage facilities [Heath et al., 2015]. Within compressor stations, reciprocating compressors are the dominant equipment level emission source [Zimmerle et al., 2015], with rod packing seal leakage among the largest individual emission sources on these units [U.S. Environmental Protection Agency, 2026a]. This makes the development of size-resolved emission frameworks for reciprocating units a high-value target for emissions estimation and reduction. Three compressor types dominate upstream and midstream natural gas applications: reciprocating, centrifugal, and oil-flooded rotary screw, with reciprocating compressors being the most numerous in U.S. natural gas operations [Piggott et al., 2021, U.S. Environmental Protection Agency, 2017, Zimmerle et al., 2020]. Reciprocating compressors have the most versatile use cases, with units ranging from less than 400 HP for production-scale vapor recovery service to over 12,000 HP for larger industrial applications, and discharge pressures from atmospheric to greater than 10,000 psig in multistage configurations [Piggott et al., 2021]. Centrifugal compressors are often selected for high-volume continuous flow usage, with single-stage compression ratios of 1.6–2.3 and gas turbine-driven pipeline units typically rated 7,000–40,000 BHP [Piggott et al., 2021, Brun, 2018]; oil-flooded rotary screw compressors handle small-to-medium flows with high compression ratios (up to 20:1) but discharge pressure limited to approximately 400 psig, most commonly in vapor recovery and refrigeration service [Piggott et al., 2021]. Although size-based emission profiling is needed for all three compressor types (because traditional emission factors do not account for unit scale), this work uses reciprocating compressors as the example system because of the extensive publicly available dataset collected in the 2017 Gathering Emission Factor (GEF) study [Zimmerle et al., 2020], which pairs component-level emission measurements with gas throughput for this type of compressor.

Reciprocating compressors generate pressure for a gas stream by using positive displacement actuated by one or more piston rods [U.S. Environmental Protection Agency, 2017]. For each suction stroke, gas enters a cylinder and then undergoes compaction by the rod, and is subsequently discharged to the existing stream [Piggott et al., 2021]. These compressor units are predominantly driven by natural-gas-fired internal combustion engines, classified by AP-42 into three types: two-stroke lean-burn (2SLB), four-stroke lean-burn (4SLB), and four-stroke rich-burn (4SRB) [U.S. Environmental Protection Agency, 2024d, Vaughn et al., 2020]. Methane emissions arise from both the driver side and the compressor side of these units, and can be classified as one of three types: combustion, vented, and fugitive. On the driver side, unburned methane entrained in engine exhaust (termed ”combustion slip”) represents a distinct combustion-category emission source [Vaughn et al., 2020]; driver-side emissions are well-characterized for the typical engines deployed on natural gas compressor systems [Johnson et al., 2015] and are used in this work as inputs to isolate compressor-side emissions, rather than as a study target. On the compressor side, the majority of emissions during normal operation are vented leakage through the rod packing system, originating from the sealing components that surround the piston rod [U.S. Environmental Protection Agency, 2017, Zimmerle et al., 2015]. During each stroke, some gas escapes around the flexible sealing cups used to maintain the pressure boundary. Over time, sealing rings degrade and emit at progressively greater rates until the seal components fail and require replacement, with emission rates clustering near a practical maximum at the upper end of the observed distribution (Section 3.1). The U.S. EPA estimates that in 2017, there were more than 51,000 reciprocating compressors in operation, housing over 200,000 rod packing systems [U.S. Environmental Protection Agency, 2017].

A major contributor to the vented emissions from reciprocating compressors is the aforementioned leakage from degrading rod packing seals, which can be modeled in relation to three different equipment states: operating (OP), not operating pressurized (NOP), and not operating depressurized (NOD) [U.S. Environmental Protection Agency, 2024c]. Rod packing leakage is categorized as vented during normal operation (OP) and fugitive in non-operating states (NOP and NOD), with OP emissions considerably more intense due to active cylinder pressure driving gas past the seal [U.S. Environmental Protection Agency, 2024c]. New rod packing typically leaks around 11–12 scfh, rising to 24–150 scfh as rings wear, with extreme cases approaching 900 scfh [Climate and Clean Air Coalition Oil and Gas Methane Partnership, 2017]. These ranges apply to large high-pressure units and are not stratified by compressor size. The current regulatory trigger for mandatory seal replacement is 2 scfm per cylinder regardless of compressor size or rated power [U.S. Environmental Protection Agency, 2024a], a size-agnostic threshold that imposes very different burdens relative to throughput depending on unit size, a limitation this work addresses directly through fractional loss.

Another common emission source is leakage through blowdown valves. A blowdown vent is a dedicated outlet line on the compressor unit which enables operators to safely discharge high volumes of gas for maintenance activities. Instances of blowdown events include inspection and/or replacement of rod packing seal rings, and the depressurization release to atmosphere results in distinct, known emission events. Outside of these maintenance events however, the blowdown valve itself can leak gas past its closed seat during normal operation, producing a continuous low-rate emission through the same vent line. This fugitive leakage through the blowdown vent is separate from intentional blowdown maintenance events, and represents a unique emission source on reciprocating compressor units, which is the blowdown-related source profiled in this work.

Field measurements at compressor stations have identified blowdown vent lines and rod packing seal vents as two of the largest emission sources among reciprocating compressor components [URS Corporation and University of Texas at Austin, 2011, U.S. Environmental Protection Agency, Office of Air Quality Planning and Standards, 2014], with rod packing systems typically emitting the highest volume of gas for compressors in good repair [Climate and Clean Air Coalition Oil and Gas Methane Partnership, 2017]. In the transmission and storage sector, major compressor equipment (rod packing vents, blowdown and isolation valves, and seal vents) accounts for approximately 50% of station fugitive emissions, which themselves represent 75% of total station methane emissions [Zimmerle et al., 2015].

Despite the frequency of leaks from rod packing and blowdown vents, there is currently no established framework for estimating 'normal' emission rates from these two leak sources as a function of compressor size. Such a framework can enable operators to distinguish normal seal wear from conditions warranting maintenance intervention.

This work demonstrates that fractional loss varies considerably across compressors of different rated power, with smaller compressors losing a disproportionately larger fraction of gas throughput from both rod packing seal vents and blowdown vents. To establish this, we characterize emission rate distributions for these two fugitive leak sources on reciprocating compressors, normalized by gas throughput to produce fractional loss distributions from the Gathering Emission Factor (GEF) gathering and boosting field study [Zimmerle et al., 2020], in which component-level emission measurements were collected at 180 gathering and boosting stations across 11 U.S. states during 2017. From these distributions, we construct a predictive model that enables operators or other interested parties to assess the likelihood of seal degradation or maintenance need by comparing an observed emission rate to the expected range for a compressor of that size. The resulting framework is evaluated against measurement-derived estimates from the Colorado Ongoing Basin Emissions (COBE) study [Brown et al., 2025], a Colorado-wide aerial inventory campaign in which three vendor platforms collected facility-level methane measurements across upstream oil and gas operations. Although COBE did not target reciprocating compressors specifically, its broad coverage captured a large number of these units, making it a useful independent dataset for comparison against the GEF-derived predictions.

Currently, there are no established methods for evaluating equipment conditions based on throughput normalized emission estimates for seal vent and blowdown vent leaks on reciprocating compressors in the field. Generally, to estimate expected emissions from these sources, emission factors are used with an activity basis of compressor count [U.S. Environmental Protection Agency, 2024b] or number of cylinders [U.S. Environmental Protection Agency, Office of Air Quality Planning and Standards, 2014, Climate and Clean Air Coalition Oil and Gas Methane Partnership, 2017]. Regulations follow this accordingly, with rod packing seal replacement required once measured emissions exceed 2 scfm per cylinder, regardless of compressor size or operating conditions [U.S. Environmental Protection Agency, 2024a]. Field measurement campaigns have produced empirical distributions of rod packing and blowdown emissions across the natural gas supply chain [Zimmerle et al., 2015, Zimmerle et al., 2020], but these distributions are reported as absolute emission rates per source, without stratification by compressor rated power or normalization by gas throughput. Using absolute emission rates to assess seal conditions does not account for emission rate dependency on associated engine size, the consequences of which are quantified in Section 3.1: smaller compressors exhibit median fractional loss several times higher than larger units across both rod packing and blowdown sources, large enough that any size-agnostic threshold will systematically misclassify equipment condition at the size (rated power) extremes. The following investigation shows that fractional loss exhibits significant variation over compressors of different rated power, which can be modeled using a log-log linear fit to GEF field measurements; percentile bands drawn from this fit define a predictive model that flags expected equipment failures leading to excess vent leakage.

In the remainder of the text, Section 2 (methods) describes the GEF dataset, the fractional loss methodology, the predictive model construction, and the COBE validation framework. Section 3 (results and discussion) presents the fractional loss distributions, the COBE comparison results, and the predictive model, and closes with a summary of findings, limitations, and directions for future work.

This section describes the methodology used to characterize size-dependent emission distributions for reciprocating compressor seal vents and blowdown vents. Fractional loss distributions are derived from field measurements collected during the GEF study described in Section 2.1, stratified by compressor rated power, and extended to non-operating states through ratio-based scaling. A predictive model is constructed from these distributions to enable assessment of seal condition as a function of compressor size. The resulting emission estimates are then compared against independent measurement-derived estimates from the COBE study, using a residual attribution method to isolate compressor-side emissions from total equipment-level measurements (Section 2.5).

2.1 Gathering Emission Factor (GEF) Study

The primary source of compressor emission data used in this work is the GEF study conducted by Zimmerle et al. [Zimmerle et al., 2020, Zimmerle et al., 2019]. In partnership with nine midstream natural gas companies, field measurements were collected at 180 gathering and boosting stations across 11 U.S. states during June through November 2017. The GEF dataset remains the most comprehensive publicly available characterization of reciprocating compressor emissions in the gathering and boosting sector, and we are aware of no subsequent peer-reviewed evidence of fleet-level shifts in rod packing or blowdown emission characteristics in this sector since the 2017 collection window. The measured stations were sampled from a population of 1,705 partner facilities located in 28 American Association of Petroleum Geologists (AAPG)-defined basins, which collectively account for approximately 85% of annual U.S. natural gas production [Zimmerle et al., 2019].

Fugitive and vented emissions were identified at the component level using optical gas imaging (OGI) cameras and quantified using a Bacharach Hi Flow Sampler, with anti-static calibrated bags used for sources exceeding the sampler's capacity [Zimmerle et al., 2019]. The dataset includes 487 reciprocating compressor observations, with emission measurements recorded for rod packing seal vents in the operating (OP), non-operating pressurized (NOP), and non-operating depressurized (NOD) states, as well as blowdown vent emissions. For each measured compressor, the dataset also provides rated horsepower and facility-level throughput as reported by participating operators; throughput data was available for 160 of the reciprocating compressor facilities visited in the field campaign [Zimmerle et al., 2020]. The GEF final report and its supplemental materials do not specify the recording or calculation methodology underlying the operator-reported throughput values, and this analysis assumes the reported values are accurate as provided. Because the fractional loss methodology described in Section 2.2 requires throughput data at the facility level, observations from facilities lacking reported throughput were excluded from the analysis. After this filtering step, 359 rod packing OP measurements from 89 facilities, 21 NOP measurements from 11 facilities, 8 NOD measurements from 5 facilities, and 88 blowdown measurements from 56 facilities were retained. The distribution of retained measurements by source and compressor HP size class is summarized in Table 1.

The GEF study is representative of the gathering and boosting sector, where compressors tend to operate at higher power ratings than those used in upstream production. Of the rod packing measurements retained for analysis, 90.3% come from compressors rated at or above 1000 HP, with the remaining 9.7% drawn from units between 200 and 1000 HP; no compressors below 200 HP were measured. Blowdown measurements are more evenly split, with 62.5% from compressors at or above 1000 HP. This size distribution is relevant to the present work because the target application, production-scale vapor recovery unit (VRU)s, typically operates in the 50–350 HP range, which is below the bulk of the GEF sampled population. Despite the difference in scale, the underlying mechanism for achieving compression is shared across applications. The U.S. EPA Natural Gas STAR Program identifies reciprocating compressors as common to production, gathering and boosting, processing, transmission, and storage operations, and describes a single rod packing system architecture (piston rod, flexible packing rings, packing cups, nose gasket, and vent stack via the packing flange or distance piece) to be applicable across all of these sectors [U.S. Environmental Protection Agency, 2026a]. The compressor at the core of a VRU is itself typically a reciprocating unit, sized to handle low-suction-pressure vapor streams from production tank batteries [U.S. Environmental Protection Agency, 2026b]. The leak pathways for the two emission sources characterized here, rod packing seal vents and blowdown vents, are therefore mechanically identical between VRU and gathering applications. What differs is scale (cylinder size, rated power, and throughput) and duty cycle, with VRUs typically handling lower-volume, more intermittent gas streams from production tank vapors. Because fractional loss normalizes by throughput, the size-dependent FL distributions developed from GEF data are appropriate to extend to the VRU size range provided the underlying seal and blowdown leak mechanisms remain the same, which the shared architecture documented by the EPA supports.

Table 1: Summary of emission measurements from the GEF study by source and compressor HP size class, after filtering for facilities with complete throughput data required for fractional loss analysis. Multiple measurements were collected per facility where applicable.

Emission Source	**Measurements**	**Facilities (All)**	**Facilities (<1000 HP)**	**Facilities (≥1000 HP)**
Rod Packing (OP)	359	89	16	73
Rod Packing (NOP)	21	11	1	10
Rod Packing (NOD)	8	5	1	4
Blowdown	88	56	26	30

2.2 Fractional Loss Distributions

From the Zimmerle et al. study, fractional loss is calculated for a population of reciprocating compressors of varying rated power and throughput. Traditional emission factors assign a single emission rate to all compressors regardless of size, but absolute emission rates are not necessarily proportional to throughput. A larger compressor operating normally may emit more methane in absolute terms than a smaller compressor with a severely degraded seal, simply because it processes more gas. Without normalizing by throughput, identifying whether a given emission rate reflects normal operation or seal degradation is ambiguous and non-diagnostic. Fractional loss, a dimensionless quantity, addresses this by expressing emissions as a fraction of gas throughput, producing a size-agnostic metric that enables direct comparison of seal condition across compressors of different rated power.

To calculate fractional loss for a given compressor, both an emission rate and a throughput value must be known. Fractional loss is defined as the ratio of the measured methane emission rate to the gas throughput:

$$\text{FL} = \frac{\text{Emission Rate (scfh)}}{\dot{m}} \tag{1}$$

where $\dot{m}$ is the volumetric throughput of gas (scfh).

The emission rate is obtained directly from field measurement, but throughput is not directly reported for many facilities (such as those part of the COBE project compared below); it can instead be estimated from the compressor rated power and the specific enthalpy change of the gas stream across the compressor.

This throughput estimate follows from the steady-flow energy balance (the first law of thermodynamics for an open system). For a control volume around the compressor, the rate of energy transfer by heat and work balances the change in the gas stream's enthalpy, kinetic energy, and potential energy:

$$\dot{Q} - \dot{W} = \dot{m}\left(\Delta h + \cancelto{0}{\tfrac{1}{2}\Delta V^2} + \cancelto{0}{g\Delta z}\right) \tag{2}$$

where $\dot{Q}$ is the rate of heat transfer to the gas (kJ/hr), $\dot{W}$ is the rate of work done by the gas (kJ/hr), $\dot{m}$ is the volumetric throughput (scfh), Δh is the specific enthalpy rise across the compressor (kJ/scf), and the final two terms are the changes in specific kinetic and potential energy. Treating compression as adiabatic sets $\dot{Q} = 0$, and the kinetic and potential energy changes across the compressor are negligible relative to the enthalpy rise. Defining the compression power as the work delivered to the gas, $\dot{W}_{\text{c}} = -\dot{W}$, the balance reduces to $\dot{W}_{\text{c}} = \dot{m}\,\Delta h$. Expressing the enthalpy rise on a per-standard-cubic-foot basis rather than per unit mass folds the gas composition and standard-state molar volume into Δh, which is evaluated thermodynamically using a real-gas equation of state for the specified gas composition and stage pressure conditions.

The compression power is taken to be the compressor's rated power, which assumes operation at full rated load. Because rated power is reported in horsepower, it is converted to a consistent energy-rate basis with $C = 2684.5$ kJ/hr/HP (equivalently 1 HP = 745.7 W). Substituting $\dot{W}_c = P_{\text{comp}} \cdot C$ into the energy balance and solving for throughput gives Equation 3, allowing throughput to be estimated from rated power and gas composition alone, without a direct flow measurement.

$$\dot{m} = \frac{P_{\text{comp}} \cdot C}{\Delta h} \tag{3}$$

where $\dot{m}$ is the volumetric throughput of gas (scfh), P_{comp} is the compressor rated power (HP), Δh is the specific enthalpy change of the gas stream across the compressor (kJ/scf), and $C = 2684.5$ kJ/hr/HP is the unit conversion factor from HP to kJ/hr.

Equation 3 assumes ideal (isentropic) compression at full rated load. Because reciprocating compressors instead operate at isentropic efficiencies of roughly 0.70–0.90 and often below full rated load, Equation 3 overestimates throughput and therefore underestimates any fractional loss computed from an estimated throughput (as in the COBE comparison) by a factor of approximately $1/(\eta\,\text{LF})$ — about 1.1–1.4 from efficiency alone, and larger once below-rated load is included, where η is the isentropic efficiency and LF the load factor. This bias is approximately size-independent, so it acts as a uniform vertical offset on the log-log axes without altering the size-dependent trend; the GEF fractional-loss distributions and the percentile model derived from them are unaffected, as they use operator-reported throughput.

Specific enthalpy change Δh is typically not a quantity readily available to operators, and it can not be measured directly on a compressor. It can however be evaluated thermodynamically using the gas composition and suction and discharge pressures. Here, Δh is taken as the isentropic enthalpy rise (evaluated at constant entropy, $s_{\text{out}} = s_{\text{in}}$) between the compressor suction state and pipeline discharge pressure, computed with the GERG-2008 equation of state [Kunz and Wagner, 2012] as implemented in NIST REFPROP v10 [Lemmon et al., 2018]. For estimating Δh associated with COBE data, the gas stream is modeled as a representative multicomponent associated gas at suction conditions of 110°F and 74.65 psia compressed to pipeline pressure, yielding $\Delta h = 14.74$ kJ/scf. Because per-facility conditions are not resolved in the COBE metadata, this single value is applied across all COBE facilities, a simplification addressed in Section 3.4.

Throughput and emission rates are both expressed in standard cubic feet (scf), referenced to 60°F and 14.696 psia following standard U.S. natural gas convention. Because fractional loss is the ratio of two volumetric flow rates expressed at the same standard reference (Equation 1), the choice of reference state enters the numerator and denominator identically and cancels, leaving the reported fractional-loss values insensitive to it.

For each facility with both emission measurements and throughput data, fractional loss was computed by dividing the facility's emission-rate distribution by its throughput. These facility-level FL distributions were then aggregated within the <1000 HP and ≥1000 HP compressor classes to produce empirical cumulative distribution functions (CDF) representing the probability of observing a given FL value in each HP size category. The distribution of scaled emission factors for a target compressor with known throughput is then:

$$\text{Scaled EF}_{\text{Rod Packing OP}} = \text{FL}_{\text{Rod Packing OP}} \cdot \dot{m} \tag{4}$$

$$\text{Scaled EF}_{\text{Blowdowns}} = \text{FL}_{\text{Blowdowns}} \cdot \dot{m} \tag{5}$$

Equations 4 and 5 apply directly to rod packing (OP) and blowdown emissions because these sources scale with throughput. However, rod packing emissions that arise in states NOP and NOD require a different approach.

2.3 Estimating rod-packing emissions for NOP and NOD states

Emissions from rod-packing systems occur in all three operating states (OP, NOP, NOD), and each originate from the same physical mechanism: methane leakage past worn piston rod seals. The emission rate differs between states due to pressure conditions, but the leak pathway remains identical. When the compressor is operating (OP), cylinder pressure drives gas through seal imperfections at the highest rate. In the non-operating pressurized (NOP) state, residual system pressure maintains some leakage. In the non-operating depressurized (NOD) state, minimal pressure differential results in very low emissions. Across all operating states, emissions increase as the seal rings/cups become worn, until the seal components fail and emission rate reaches a maximum.

Table 1 reveals a data limitation: only one facility in the <1000 HP category contributes NOP measurements, and only one contributes NOD measurements. This is insufficient to characterize the FL distribution shape for these states. However, across all facilities (both HP size classes), consistent emission ratios emerge (Table 2):

$$\text{Avg. Emissions}_{\text{OP}} = \frac{1}{n}\sum_{i=1}^{n} e_{\text{op},i} \tag{6}$$

$$\text{Avg. Emissions}_{\text{NOP}} = \frac{1}{n}\sum_{i=1}^{n} e_{\text{nop},i} \tag{7}$$

$$\text{Avg. Emissions}_{\text{NOD}} = \frac{1}{n}\sum_{i=1}^{n} e_{\text{nod},i} \tag{8}$$

where $e_{\text{op},i}$, $e_{\text{nop},i}$, and $e_{\text{nod},i}$ denote the measured emission rates (scfh) for a given facility i in each respective operating state, and n is the number of facilities contributing measurements in that state.

Table 2: Mean rod packing emission rate in each operating state and each non-operating state's ratio to the operating-state mean, computed across all GEF facilities reporting emissions in that state. Because these ratios depend only on emission rate and not throughput, this facility set is larger than the throughput-filtered set in Table 1.

Operating State	**Mean Emission Rate (scfh)**	**Facilities**	**Ratio to OP**
OP	122	101	1
NOP	2.74	12	0.0226
NOD	0.31	5	0.0025

The NOP/OP and NOD/OP ratios computed from Equations 7 and 8 represent the dataset-wide average emissions in each non-operating state as a single multiplicative factor relative to the operating state. Since direct measurements in these states are too sparse to characterize a distribution independently, each ratio (a scalar quantity) is multiplied by the OP fractional loss distribution, shifting it downward to reflect the lower pressure conditions in each non-operating state, while preserving the shape of the well-sampled OP population. This approach allows the variability captured in the OP measurements (across 89 facilities and 359 measurements) to inform the shape of the NOP and NOD distributions, where direct measurement coverage is limited to 21 and 8 measurements respectively (Table 1). The corresponding distributions of scaled emission factor for a target compressor are:

$$\text{Scaled EF}_{\text{Rod Packing NOP}} = \left(\frac{\text{Avg. Emissions}_{\text{NOP}}}{\text{Avg. Emissions}_{\text{OP}}}\right) \cdot \text{Scaled EF}_{\text{Rod Packing OP}} \tag{9}$$

$$\text{Scaled EF}_{\text{Rod Packing NOD}} = \left(\frac{\text{Avg. Emissions}_{\text{NOD}}}{\text{Avg. Emissions}_{\text{OP}}}\right) \cdot \text{Scaled EF}_{\text{Rod Packing OP}} \tag{10}$$

This approach relies on two assumptions that cannot be empirically verified given current sample sizes. First, that the OP distribution shape is a reasonable proxy for the NOP and NOD distribution shapes. Second, that the NOP/OP and NOD/OP ratios computed from the pooled GEF dataset apply uniformly across compressor sizes. The physical basis for both assumptions is that all three operating states involve methane leakage past the same physical seal components (rod packing rings, packing cups, nose gasket) along the same leak pathway, with the operating state determining only the magnitude of the pressure differential driving the leak [U.S. Environmental Protection Agency, 2026a]. Because seal condition (fit, alignment, and wear) governs the variability in fractional loss across the population, and seal condition is independent of operating state, the OP shape is expected to carry over to NOP and NOD. The size-independence of the ratios is a less verifiable assumption and is acknowledged as a limitation in Section 3.4.

2.4 Predictive Model

To relate fractional loss to compressor size continuously rather than by discrete HP class, a linear model was fit to the GEF rod packing (OP) measurements in log-log space:

$$\log_{10}(\text{FL}) = a + b \cdot \log_{10}(\text{HP}) \tag{11}$$

yielding $a = -0.334$ and $b = -1.592$ ($n = 359$). Percentile bands were assembled from the distribution of residuals about this fit line, producing parallel lines on the log-log axes at the 5th, 25th, 50th, 75th, 80th, 90th, and 95th percentiles (denoted P5, P25, P50, P75, P80, P90, and P95, respectively). These bands constitute a simple model for compressor seal condition that bins the FL-HP space into categories ranging from low emitters (P5–P25) to likely failing seals (above P90).

2.5 COBE Study Comparison

The Colorado Ongoing Basin Emissions (COBE) study was a regional investigation that estimated methane emissions for upstream oil and gas facilities across Colorado. Three aerial sensor companies were contracted to collect measurements statewide: Bridger Photonics, deploying their Gas Mapping LiDAR (GML 2.0) system; GHGSat, deploying three DATA AIR sensors (AV1, AV3, and AV5) that use shortwave infrared spectrometry; and Insight M, deploying two LeakSurveyor hyperspectral infrared sensors. Further details on each platform are provided in the COBE final report [Brown et al., 2025]. Across all three vendors, 2,102 emission detections were identified. Detections exceeding 2 kg/hr were subject to a source cause resolution process by the COBE modeling team, supplemented by review of aerial imagery and operator records when available [Brown et al., 2025]. As part of this process, MAES (described in Section 2.6) was used to estimate driver-side exhaust emissions on a per-facility basis using rated power, engine class, and other facility-specific parameters. The present work uses these MAES-derived driver exhaust estimates to isolate compressor-side emissions via the residual method described below.

Direct measurements of rod packing seal vent emissions were not available from the COBE dataset, but were estimated by subtracting known engine-side emissions from the total aerial measurement. Crankcase ventilation (CCV) emissions were estimated as a fixed fraction of driver exhaust:

$$\dot{E}_{\text{RP,residual}} = \dot{E}_{\text{measured}} - \dot{E}_{\text{DE}} - \dot{E}_{\text{CCV}} \tag{12}$$

$$\dot{E}_{\text{CCV}} = 0.144 \cdot \dot{E}_{\text{DE}} \tag{13}$$

where $\dot{E}_{\text{CCV}}$ is the methane emission rate from crankcase ventilation (scfh), $\dot{E}_{\text{DE}}$ is the methane emission rate from driver exhaust (scfh), and the coefficient 0.144 represents the average ratio of crankcase-to-exhaust methane emissions measured for four-stroke lean-burn engines operating under typical field conditions [Johnson et al., 2015]; this ratio implicitly reflects the combustion efficiency of the measured engines and may vary across units with different loading or maintenance history. The estimated compressor-side emission rate is then:

$$\dot{E}_{\text{RP,residual}} = \dot{E}_{\text{measured}} - 1.144 \cdot \dot{E}_{\text{DE}} \tag{14}$$

where $\dot{E}_{\text{RP,residual}}$ is the rod packing residual methane emission rate (scfh), defined as the portion of the aerial measurement remaining after driver-side emissions are subtracted and attributed to rod packing seal vents despite potentially containing contributions from other compressor-side sources, $\dot{E}_{\text{measured}}$ is the total methane emission rate observed by the aerial platform (scfh), and the factor 1.144 combines driver exhaust and crankcase ventilation contributions per Equation 13.

This residual includes contributions from rod packing seal vents as well as other compressor-side sources such as component leaks and pneumatic vents, which are not separately resolved. For each COBE facility with a detected compressor emission, throughput was estimated from the rated horsepower reported in the COBE facility metadata using Equation 3, with a stage 2 gas composition assumption ($\Delta h = 14.74$ kJ/scf). Fractional loss was then computed as the ratio of the residual emission rate to estimated throughput (Equation 1).

The resulting COBE fractional loss values were compared against the GEF prediction bands (Section 2.4) as a qualitative consistency check. Because the COBE aerial platforms had substantially higher detection limits than the high-flow samplers used in the GEF field campaign, COBE detections were expected to preferentially capture compressors with elevated emissions, and should therefore fall in the upper tail of the GEF-derived distribution.

2.6 MAES Compressor Model

The Mechanistic Air Emissions Simulator (MAES) is a discrete event simulator used to model emissions from oil and gas equipment at the site level. In the COBE study, MAES generates expected emission profiles for each facility, which serve as the baseline against which measurement-derived estimates are compared during the cause analysis process described in Section 2.5.

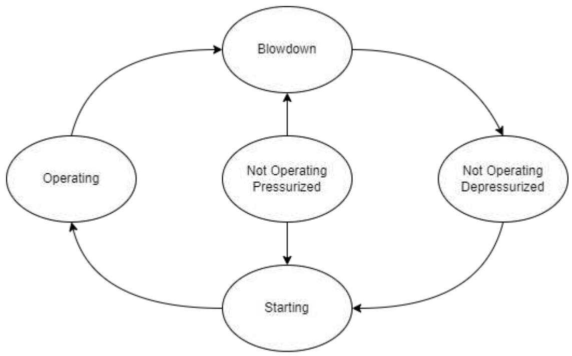

Figure 1: Operational states represented in the MAES compressor model for reciprocating compressor units.

The MAES compressor model represents each unit as occupying one of five operational states: operating (OP), not operating pressurized (NOP), not operating depressurized (NOD), starting, and blowdown. Transitions between states are governed by a Markov chain parameterized by operating fraction, NOP/NOD split, and operating duration bounds specified in the site definition. Monte Carlo iterations are used to propagate uncertainty through the simulation. Each reciprocating compressor unit is assumed to have one rod packing vent, one single unit vent, one blowdown valve, one starter valve, and two isolation valves (one inlet and one outlet), consistent with the standard single-unit architecture defined under EPA Subpart W [U.S. Environmental Protection Agency, 2024c]. For multi-cylinder units, the rod packing vent represents the manifolded aggregate of all cylinder vents.

Given this assumed layout, the model resolves emissions at the individual emitter level. Rod packing seal vent emissions are modeled separately for each operating state (OP, NOP, NOD), with OP emissions classified as vented and NOP/NOD emissions classified as fugitive, all driven by the state-specific pressure differential across the rod packing seal. Blowdown vent leaks, component leaks, pneumatic device vents, and driver exhaust (combustion slip) are each modeled by MAES as distinct emitters as well. Driver exhaust emissions are computed from rated power, engine type (2SLB, 4SLB, 4SRB, or turbine), average loading, and engine efficiency. Each emitter references a gas composition file and an emission factor set, enabling site-specific configurations. As described in Section 2.5, the present work uses MAES only to obtain per-compressor driver exhaust estimates that feed Equation 14.

3.1 Fractional loss distributions from GEF field data

Fractional loss distributions were calculated for rod packing and blowdown vent emissions from the GEF study, stratified by compressor rated power above and below 1000 HP. Figures 2 and 3 display fractional loss compared to associated compressor power rating for both leak sources. Both show a general decrease in fractional loss with increasing HP, with wide variability spanning several orders of magnitude within each HP size class. This spread of observed emission rates reflects the population of seal condition states present in a typical field measurement campaign: a randomly sampled compressor may be operating with newly installed packing, with progressively worn rings, or near a maintenance threshold, and these conditions exhibit the full range of expected leak rates for a given compressor size [Climate and Clean Air Coalition Oil and Gas Methane Partnership, 2017]. Operating conditions, gas composition, and operator maintenance practices also contribute, but seal condition is expected to be the dominant source of within-class variability given the wide emission range associated with progressive packing degradation.

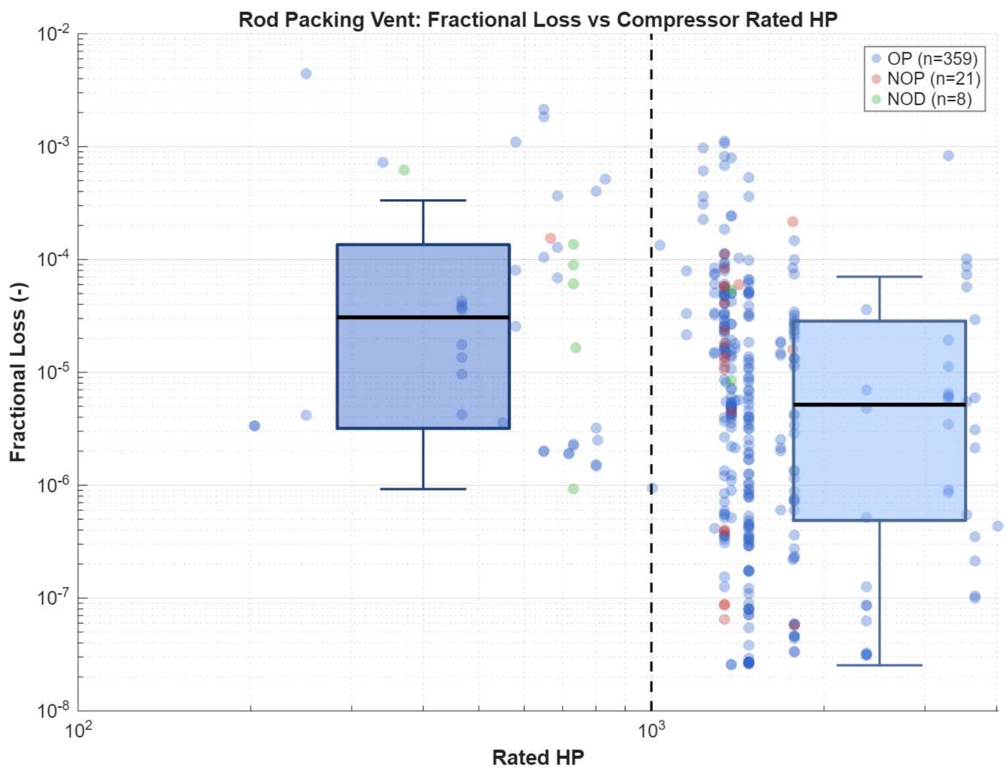

Figure 2: Fractional loss versus compressor rated power for rod packing vent emissions (OP, NOP, and NOD combined) from the GEF field study. Individual measurements are shown as scatter points on log-log axes, with overlaid box plots summarizing the distribution within each HP class. The dashed vertical line marks the 1000 HP stratification boundary. Compressors below 1000 HP (n=42 measurements) exhibit a median fractional loss of 3.07×10^{-5}, approximately six times higher than compressors at or above 1000 HP (n=346 measurements, median 5.17×10^{-6}). Measurements span several orders of magnitude within each HP class, reflecting wide variability in seal condition, maintenance history, and operating practices.

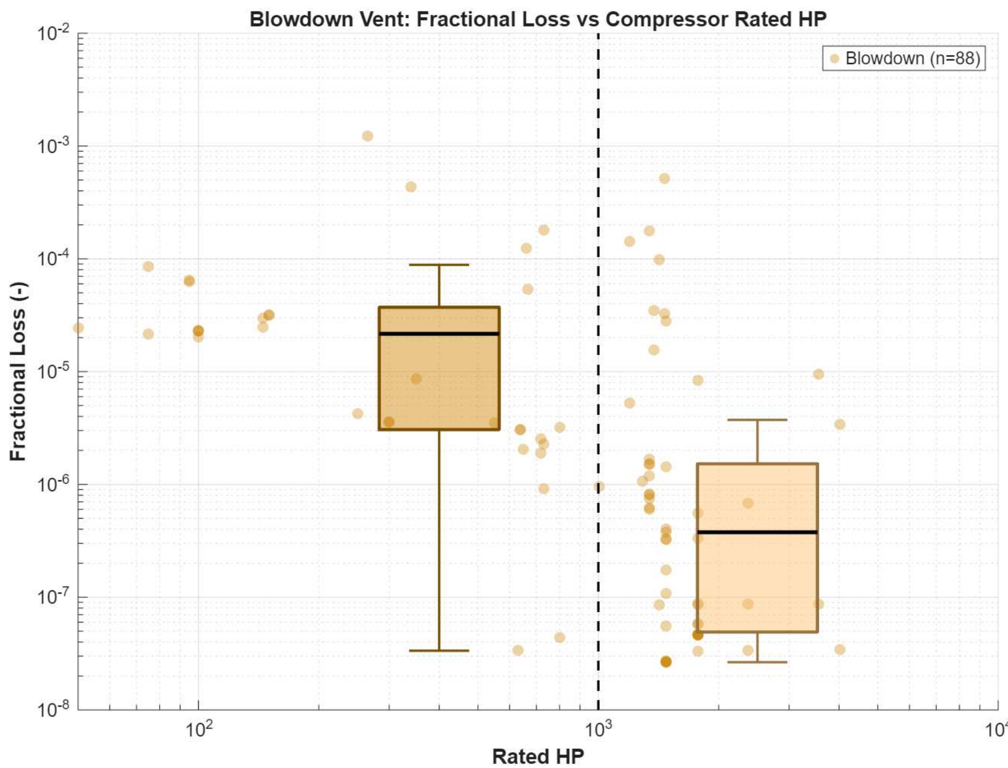

Figure 3: Fractional loss versus compressor rated power for blowdown vent emissions from the GEF field study. Individual measurements are shown as scatter points on log-log axes, with overlaid box plots summarizing the distribution within each HP class. The dashed vertical line marks the 1000 HP stratification boundary. Compressors below 1000 HP (n=33 measurements, median 2.16×10^{-5}) show median fractional loss roughly 57 times that of the larger class (n=55 measurements, median 3.76×10^{-7}). Measurements span several orders of magnitude within each HP class, reflecting wide variability in seal condition, maintenance history, and operating practices. This variability motivates the use of HP-stratified fractional loss distributions rather than single-valued emission factors.

Figure 4 presents the empirical CDFs for rod packing emissions in the operating (OP) state, the only state with sufficient sample size to characterize the FL distribution shape directly. Compressors rated below 1000 HP (n=16 facilities) exhibit a median fractional loss of 1.77×10^{-5}, approximately 3.6 times higher than compressors rated at or above 1000 HP (n=73 facilities, median 4.85×10^{-6}). The rightward shift of the smaller compressor distribution indicates systematically higher emissions per unit throughput across the entire probability range.

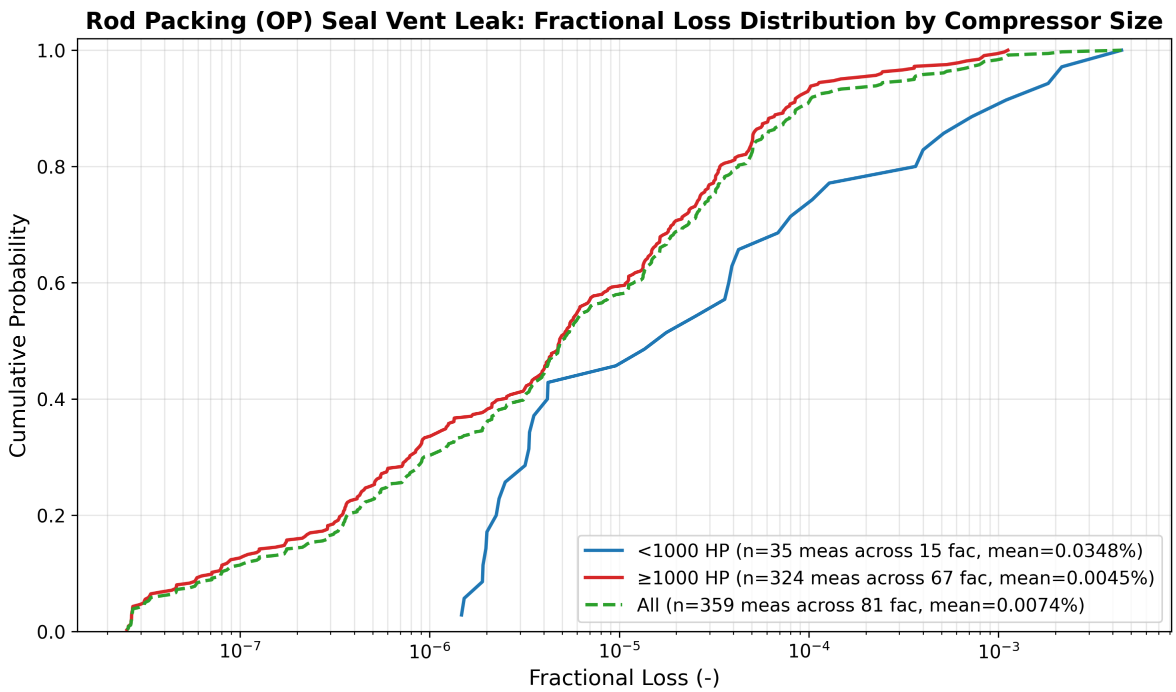

Figure 4: Empirical cumulative distribution functions of fractional loss for rod packing operating (OP) emissions, stratified by compressor rated power. Compressors below 1000 HP (blue, n=35 measurements across 15 facilities, median FL = 1.77×10^{-5}) exhibit substantially higher fractional loss than those at or above 1000 HP (red, n=324 measurements across 67 facilities, median FL = 4.85×10^{-6}). The dashed green curve represents the combined population (n=359 measurements across 81 unique facilities; one facility operates compressors in both HP classes and is counted once per class, median FL = 4.98×10^{-6}).

A similar pattern is observed for blowdown vent emissions (Figure 5). Compressors below 1000 HP (n=26 facilities) have a median blowdown fractional loss of 2.16×10^{-5}, compared to 3.76×10^{-7} for compressors at or above 1000 HP (n=30 facilities), a median ratio of approximately 57. The corresponding mean ratio is far smaller, approximately 3.9; this divergence reflects the heavy right-skew of the blowdown distribution, most pronounced in the ≥1000 HP class, where a small number of high-emitting compressors inflate the class mean and pull it to within roughly a factor of four of the smaller class, even as the two class medians remain about 57 times apart. While the absolute magnitude of blowdown fractional loss is lower than that of rod packing emissions, the size-dependent separation is consistent across both source types, indicating that smaller compressors lose a greater fraction of throughput to both seal degradation and blowdown pathways. This pattern does not depend on the specific choice of 1000 HP as the stratification boundary. Moving the cutoff anywhere between 750 and 1250 HP preserves both the direction and the approximate magnitude of the size effect for both sources.

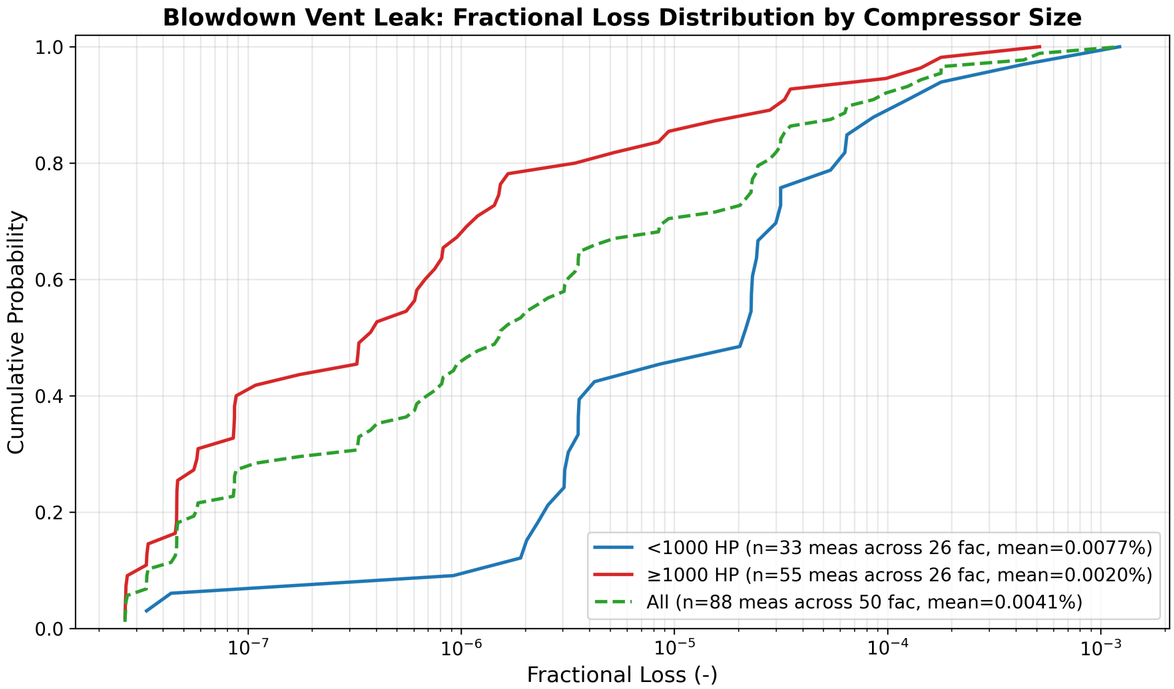

Figure 5: Empirical cumulative distribution functions of fractional loss for blowdown vent emissions, stratified by compressor rated power. Compressors below 1000 HP (blue, n=33 measurements across 26 facilities, median FL $= 2.16 \times 10^{-5}$) show higher fractional loss than those at or above 1000 HP (red, n=55 measurements across 26 facilities, median FL $= 3.76 \times 10^{-7}$). The dashed green curve represents the combined population (n=88 measurements across 50 facilities, median FL $= 1.52 \times 10^{-6}$).

Both distributions exhibit strong right-skew, most pronounced in the blowdown data. Within the ≥1000 HP blowdown class, the mean fractional loss exceeds the median by more than an order of magnitude, indicating that a small fraction of compressors contribute disproportionately to aggregate emissions. This heavy-tailed behavior is consistent with emission distributions reported elsewhere in the oil and gas methane literature [Brandt et al., 2014, Zavala-Araiza et al., 2017], and reinforces the case for reporting fractional loss distributions rather than single emission factors: the median characterizes the typical compressor, while the upper tail captures the failure or upset conditions that dominate aggregate totals.

These distributions are representative of the size-dependent emission behavior for leaks from the seal vent (Figure 4) and the blowdown vents (Figure 5) on a given compressor. For a target compressor unit with known rated power and gas composition, the appropriate size-class distribution is sampled to assign a fractional loss value, which is then multiplied by the estimated throughput to yield an emission rate. The following subsection evaluates whether these GEF-derived distributions produce emission estimates consistent with independent measurement-derived estimates.

3.2 Seal vent emissions comparison with COBE

Figure 6 displays the measurement-derived fractional loss values from the COBE dataset alongside the GEF study field measurements as a function of associated engine rated power. The distribution of COBE observations (red tones, n=90 facilities across four HP bins) are greater in magnitude relative to GEF measurements (blue tones, n=359 measurements) by approximately 1–3 orders of magnitude across the HP range. Both populations exhibit a general decreasing trend of fractional loss with increasing rated power, consistent with the size-dependent behavior established in Section 3.1, but the vertical offset between the two datasets is persistent.

There are several plausible explanations for this discrepancy. First and foremost, the aerial measurement platforms used in the COBE campaign have detection limits substantially higher than that of the high-flow samplers employed in the GEF field study. The Bacharach Hi Flow Sampler used in GEF has a nominal measurement range of 0.05–8 scfm, corresponding to approximately 0.1–10 kg/hr of methane for pipeline-quality natural gas [Howard et al., 2015]. The COBE aerial vendors have minimum detection limits spanning roughly 1 kg/hr for Bridger Photonics' Gas Mapping LiDAR [Thorpe et al., 2024] to 5–25 kg/hr for the GHGSat and Insight M systems [Brown et al., 2025]. Bridger accounted for the majority of COBE detections used in this validation, but its reliable detection threshold still exceeds the lower bound of the BHFS by roughly an order of magnitude. This introduces a selection bias: COBE preferentially captures compressors with elevated emissions, effectively truncating the lower tail of the emission distribution. Secondly, the COBE compressor population also skews toward smaller rated power than the GEF dataset; given the FL-HP trend established in Section 3.1, this compositional difference alone would push COBE-derived fractional loss upward relative to GEF data, independent of any measurement artifact. Additionally, the residual attribution method Equation 12 does not isolate rod packing emissions exclusively. The rod packing residual $\dot{E}_{\mathrm{RP,residual}}$ includes contributions from component-level fugitive leaks, pneumatic device vents, and potentially other compressor-side sources that are not subtracted in the estimation. Finally, throughput for COBE compressors is estimated using a single gas composition assumption, and variation in actual gas composition and operating conditions across Colorado facilities introduces additional uncertainty into the COBE-derived fractional loss values.

Taken together, these factors indicate that the COBE-derived fractional loss values should be interpreted as representative of the upper tail of the emission distribution, consistent with failure or anomalous operating conditions, rather than as typical seal vent performance. The concentration of COBE points near and above the P95 threshold (Figure 6) supports the use of this chart as a diagnostic tool: compressors with observed fractional loss above P95 are fitting candidates for seal inspection or replacement.

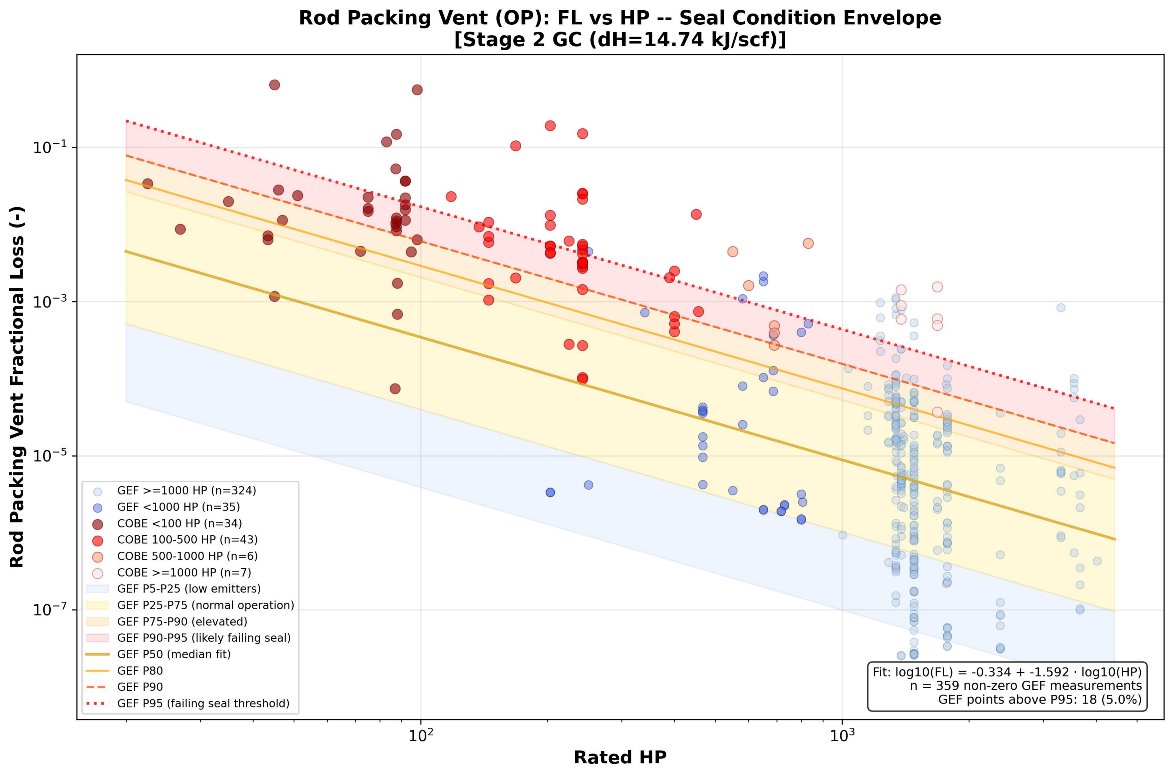

Figure 6: Rod packing vent (OP) fractional loss versus compressor rated power with seal condition expectations defined by percentile bands. A log-log linear fit to GEF field data ($\log_{10}(\text{FL}) = -0.334 - 1.592 \cdot \log_{10}(\text{HP})$, n=359) defines percentile bands representing seal condition categories: P5–P25 (low emitters, blue), P25–P75 (normal operation, yellow), P75–P90 (elevated, orange), and P90–P95 (likely failing seal, pink). The dotted red P95 line marks the failing seal threshold; 5.0% of GEF measurements exceed this line. COBE aerial measurement-derived estimates (red tones) cluster predominantly above P90, consistent with detection bias toward high-emitting and failing compressors. GEF data are stratified by HP class: $\geq$1000 HP (light blue, n=324) and $<$1000 HP (dark blue, n=35). Throughput estimated using Stage 2 gas composition ($\Delta h = 14.74$ kJ/scf).

3.3 Summary of findings

The distributions of fractional loss from rod packing seal vents and blowdown vents vary considerably across the range of reciprocating compressor sizes observed in the GEF dataset, with smaller compressors exhibiting systematically higher fractional loss than larger units for both sources, at the median and across the full distribution (Section 3.1). These results indicate that traditional emission factors, which do not account for compressor size, are insufficient to characterize seal vent and blowdown emissions across the range of compressors deployed in the oil and gas supply chain. HP-stratified fractional loss distributions provide a more physically grounded approach, capturing both the size dependence and the inherent variability in emissions within each compressor class.

Using the fractional loss distributions derived from GEF field data, a log-log linear fit (Equation 11) establishes the expected relationship between FL and rated power for fugitive rod packing seal vent emissions. Percentile bands scaled from the fit residuals define a predictive model (Figure 6) that partitions the FL-HP space into seal condition categories ranging from low/baseline emitters (P5–P25) to likely failing seals (P90–P95 and above). For a given compressor, a measured emission rate can be converted to fractional loss using rated power and estimated throughput, then located on the percentile bands to assess whether the unit is operating within normal bounds or exhibiting signs of seal degradation. This provides operators with a quantitative, HP-adjusted criterion for prioritizing maintenance, in contrast to absolute emission rate thresholds which do not account for the higher baseline emissions expected from smaller compressors.

Comparison with the measurement-derived estimates collected during the COBE inventory study provides support for this diagnostic framework. The COBE-derived rod packing seal vent fractional loss values cluster predominantly near and above the P90 line, with many exceeding the P95 threshold (Figure 6). Several factors explain why COBE observations fall in the upper tail of the GEF distribution rather than the center. Aerial sensors have minimum detection limits substantially higher than those of the high-flow samplers used in the GEF field study, biasing detections toward compressors with elevated emissions. Additionally, the residual attribution method Equation 12 does not isolate rod packing emissions exclusively, inflating the apparent fractional loss relative to what a direct seal vent measurement would yield.

3.4 Limitations

Several limitations of this analysis warrant discussion. The GEF dataset is predominantly composed of midstream compressors rated at or above 1000 HP. The $<$1000 HP subset contains 42 rod packing measurements (across OP, NOP, and NOD states) and 33 blowdown measurements, concentrated between 200 and 1000 HP, with no observations below 200 HP. The fractional loss distributions for this class are therefore extrapolated, not validated, for the production-scale vapor recovery units below 200 HP that represent part of the target application. Given the relationship observed in this study between increasing FL with decreasing HP, this may be an important HP range to characterize with additional direct measurements. Separately, GEF throughput is reported at the facility level, so where a facility operates multiple compressors manifolded to a shared gas stream, this value cannot be uniquely attributed to an individual unit, introducing uncertainty into per-compressor fractional loss.

Rod packing emissions in the NOP and NOD states are characterized using ratio-based scaling from the OP distribution (Equations 9–10), with ratios computed from the full GEF dataset. This implicitly assumes size-independent ratios between operating states, an assumption that cannot be verified with only one

<1000 HP facility contributing measurements in each state (Table 1). The physical basis for this assumption is that all three states involve leakage past the same seal components under differing pressure conditions, which requires verification.

Interpreting the comparison between predicted GEF and COBE observed emissions requires acknowledging several confounding variables. As noted above, the residual attribution method does not isolate rod packing emissions exclusively, so the COBE-derived estimate carries contributions from other compressor associated sources. Throughput for COBE compressors is also estimated from compressor rated power and a single enthalpy value (Stage 2, $\Delta h = 14.74$ kJ/scf). Because suction temperature and pressure vary across facilities in the field, this fixed value does not reflect site-specific operating conditions. Each of these simplifications introduce uncertainty into the COBE fractional loss values and thereby the diagnostic certainty. Despite the mentioned limitations, the fractional loss distributions and predictive model bands represent the best available characterization of size-dependent seal vent and blowdown emissions for reciprocating compressors, given the current state of publicly available field data.

3.5 Future work

The most pressing data need is additional field measurements of compressor emissions with associated throughput data, particularly for compressors below 300 HP, for NOP and NOD operating states, and for blowdown vent emissions. The scarcity of data in these categories is the primary constraint on the applicability of the fractional loss distributions to production-scale compressors, including VRUs.

Additional measurement comparisons from different detection solution technologies would also be valuable. The GEF field data were collected using high-flow samplers capable of measuring individual seal vents at close range, while the COBE rod packing estimates were derived from aerial platforms with fundamentally different detection characteristics. Understanding how fractional loss estimates compare across measurement technologies (high-flow sampler, optical gas imaging, aerial remote sensing) would clarify the extent to which apparent discrepancies between datasets reflect true emission differences versus measurement methodology artifacts. However, conducting a controlled cross-technology comparison for a single emission source type such as rod packing seal vents presents significant logistical challenges, as aerial campaigns are not typically designed to target individual component-level sources.

Finally, the predictive model framework developed here for reciprocating compressor seal vents and blowdown vents may be extensible to other compressor types (centrifugal, rotary screw) if analogous throughput-normalized emission data become available. The underlying principle, that fractional loss provides a size-independent metric for identifying anomalous emissions, is not specific to reciprocating compressors and could support broader application in emissions monitoring and maintenance prioritization across the oil and gas supply chain.

REFERENCES

[Alvarez et al., 2012] Alvarez, R. A., Pacala, S. W., Winebrake, J. J., Chameides, W. L., and Hamburg, S. P. (2012). Greater focus needed on methane leakage from natural gas infrastructure. Proceedings of the National Academy of Sciences, 109(17):6435–6440.

[Alvarez et al., 2018] Alvarez, R. A., Zavala-Araiza, D., Lyon, D. R., Allen, D. T., Barkley, Z. R., Brandt, A. R., Davis, K. J., Herndon, S. C., Jacob, D. J., Karion, A., Kort, E. A., Lamb, B. K., Lauvaux, T., Maasakkers, J. D., Marchese, A. J., Omara, M., Pacala, S. W., Peischl, J., Robinson, A. L., and Hamburg, S. P. (2018). Assessment of methane emissions from the U.S. oil and gas supply chain. Science, 361(6398):186–188.

[Brandt et al., 2014] Brandt, A. R., Heath, G. A., Kort, E. A., O'Sullivan, F., Pétron, G., Jordaan, S. M., Tans, P., Wilcox, J., Gopstein, A. M., Arent, D., Wofsy, S., Brown, N. J., Bradley, R., Stucky, G. D., Eardley, D., and Harriss, R. (2014). Methane Leaks from North American Natural Gas Systems. Science, 343(6172):733–735.

[Brown et al., 2025] Brown, J. A., Moy, M., Santos, A., Rimelman, E., Mollel, W., Khaliukova, O., Okenberg, C., Daniels, W. S., Hammerling, D. M., Zimmerle, D., and Hodshire, A. L. (2025). Colorado ongoing basin emissions (COBE) updated final report. Technical report, Colorado State University, Energy Institute, Fort Collins, Colorado. Prepared for Colorado Department of Public Health and Environment, Air Pollution Control Division.

[Brun, 2018] Brun, K. (2018). The US natural gas compression infrastructure: Opportunities for efficiency improvements. In University Turbine Systems Research Symposium. Elliott Group. Hosted by the National Energy Technology Laboratory.

[Climate and Clean Air Coalition Oil and Gas Methane Partnership, 2017] Climate and Clean Air Coalition Oil and Gas Methane Partnership (2017). Technical guidance document number 4: Reciprocating compressors. Technical report, Climate and Clean Air Coalition.

[Forster et al., 2021] Forster, P., Storelvmo, T., Armour, K., Collins, W., Dufresne, J.-L., Frame, D., Lunt, D. J., Mauritsen, T., Palmer, M. D., Watanabe, M., Wild, M., and Zhang, H. (2021). The Earth's Energy Budget, Climate Feedbacks, and Climate Sensitivity, pages 923–1054. Cambridge University Press, Cambridge, United Kingdom and New York, NY, USA.

[Heath et al., 2015] Heath, G., Warner, E., Steinberg, D., and Brandt, A. (2015). Estimating U.S. methane emissions from the natural gas supply chain: Approaches, uncertainties, current estimates, and future studies. Technical Report NREL/TP-6A50-62820, Joint Institute for Strategic Energy Analysis, National Renewable Energy Laboratory.

[Howard et al., 2015] Howard, T., Ferrara, T. W., and Townsend-Small, A. (2015). Sensor transition failure in the high flow sampler: Implications for methane emission inventories of natural gas infrastructure. Journal of the Air & Waste Management Association, 65(7):856–862.

[Jackson et al., 2020] Jackson, R. B., Saunois, M., Bousquet, P., Canadell, J. G., Poulter, B., Stavert, A. R., Bergamaschi, P., Niwa, Y., Segers, A., and Tsuruta, A. (2020). Increasing anthropogenic methane emissions arise equally from agricultural and fossil fuel sources. Environmental Research Letters, 15(7):071002.

[Johnson et al., 2015] Johnson, M. R., Tyner, D. R., and Szekeres, A. J. (2015). Methane emissions from leak and loss audits of natural gas compressor stations and storage facilities. Environmental Science & Technology, 49(13):8132–8139.

[Kunz and Wagner, 2012] Kunz, O. and Wagner, W. (2012). The GERG-2008 wide-range equation of state for natural gases and other mixtures: An expansion of GERG-2004. Journal of Chemical & Engineering Data, 57(11):3032–3091.

[Lemmon et al., 2018] Lemmon, E. W., Bell, I. H., Huber, M. L., and McLinden, M. O. (2018). NIST standard reference database 23: Reference fluid thermodynamic and transport properties–REFPROP, version 10.0. National Institute of Standards and Technology, Standard Reference Data Program, Gaithersburg.

[Piggott et al., 2021] Piggott, B., Mamrosh, D., Ryan, A., McKaskle, R., and Myers, D. (2021). Overview of Natural Gas Compression Options in Upstream and Midstream Operations. In Laurance Reid Gas Conditioning Conference, Norman, Oklahoma, USA. Trimeric Corporation.

[Saunois et al., 2020] Saunois, M., Stavert, A. R., Poulter, B., Bousquet, P., Canadell, J. G., Jackson, R. B., Raymond, P. A., Dlugokencky, E. J., Houweling, S., Patra, P. K., Ciais, P., Arora, V. K., Bastviken, D., Bergamaschi, P., Blake, D. R., Brailsford, G., Bruhwiler, L., Carlson, K. M., Carrol, M., Castaldi, S., Chandra, N., Crevoisier, C., Crill, P. M., Covey, K., Curry, C. L., Etiope, G., Frankenberg, C., Gedney, N., Hegglin, M. I., Höglund-Isaksson, L., Hugelius, G., Ishizawa, M., Ito, A., Janssens-Maenhout, G., Jensen, K. M., Joos, F., Kleinen, T., Krummel, P. B., Langenfelds, R. L., Laruelle, G. G., Liu, L., Machida, T., Maksyutov, S., McDonald, K. C., McNorton, J., Miller, P. A., Melton, J. R., Morino, I., Müller, J., Murguia-Flores, F., Naik, V., Niwa, Y., Noce, S., O'Doherty, S., Parker, R. J., Peng, C., Peng, S., Peters, G. P., Prigent, C., Prinn, R., Ramonet, M., Regnier, P., Riley, W. J., Rosentreter, J. A., Segers, A., Simpson, I. J., Shi, H., Smith, S. J., Steele, L. P., Thornton, B. F., Tian, H., Tohjima, Y., Tubiello, F. N., Tsuruta, A., Viovy, N., Voulgarakis, A., Weber, T. S., Van Weele, M., Van Der Werf, G. R., Weiss, R. F., Worthy, D., Wunch, D., Yin, Y., Yoshida, Y., Zhang, W., Zhang, Z., Zhao, Y., Zheng, B., Zhu, Q., Zhu, Q., and Zhuang, Q. (2020). The Global Methane Budget 2000–2017. Earth System Science Data, 12(3):1561–1623.

[Thorpe et al., 2024] Thorpe, M. J., Kreitinger, A., Altamura, D. T., Dudiak, C. D., Conrad, B. M., Tyner, D. R., Johnson, M. R., Brasseur, J. K., Roos, P. A., Kunkel, W. M., Carre-Burritt, A., Abate, J., Price, T., Yaralian, D., Kennedy, B., Newton, E., Rodriguez, E., Elfar, O. I., and Zimmerle, D. J. (2024). Deployment-invariant probability of detection characterization for aerial LiDAR methane detection. Remote Sensing of Environment, 315:114435.

[URS Corporation and University of Texas at Austin, 2011] URS Corporation and University of Texas at Austin (2011). Natural gas industry methane emission factor improvement study, final report. Technical report, U.S. Environmental Protection Agency, Office of Air and Radiation.

[U.S. Energy Information Administration, 2023] U.S. Energy Information Administration (2023). Natural gas explained: What is natural gas? https://www.eia.gov/energyexplained/natural-gas/. Accessed April 2026.

[U.S. Energy Information Administration, 2024] U.S. Energy Information Administration (2024). Total energy: Table 1.2 – Primary energy production by source. https://www.eia.gov/totalenergy/data/monthly/pdf/sec1_3.pdf. Accessed April 2026.

[U.S. Environmental Protection Agency, 2017] U.S. Environmental Protection Agency (2017). Reducing methane emissions from compressor rod packing systems.

[U.S. Environmental Protection Agency, 2024a] U.S. Environmental Protection Agency (2024a). 40 CFR 60.5393c: What GHG standards apply to reciprocating compressor designated facilities? Code of Federal Regulations, Subpart OOOOc.

[U.S. Environmental Protection Agency, 2024b] U.S. Environmental Protection Agency (2024b). 40 CFR 98.233: Calculating GHG emissions, subpart W – petroleum and natural gas systems. Code of Federal Regulations.

[U.S. Environmental Protection Agency, 2024c] U.S. Environmental Protection Agency (2024c). 40 CFR 98.238: Definitions, subpart W – petroleum and natural gas systems. Code of Federal Regulations.

[U.S. Environmental Protection Agency, 2024d] U.S. Environmental Protection Agency (2024d). Compilation of air pollutant emissions factors AP-42, section 3.2: Natural gas-fired reciprocating engines. Technical report, U.S. Environmental Protection Agency, Office of Air Quality Planning and Standards.

[U.S. Environmental Protection Agency, 2024e] U.S. Environmental Protection Agency (2024e). Understanding global warming potentials (GWPs). `https://www.epa.gov/ghgemissions/understanding-global-warming-potentials`. Accessed April 2026.

[U.S. Environmental Protection Agency, 2026a] U.S. Environmental Protection Agency (2026a). Reciprocating compressors. Natural Gas STAR Program, Methane Mitigation Technologies Platform. Last updated February 24, 2026.

[U.S. Environmental Protection Agency, 2026b] U.S. Environmental Protection Agency (2026b). Vapor recovery units. Natural Gas STAR Program, Methane Mitigation Technologies Platform. Last updated February 24, 2026.

[U.S. Environmental Protection Agency, Office of Air Quality Planning and Standards, 2014] U.S. Environmental Protection Agency, Office of Air Quality Planning and Standards (2014). Oil and natural gas sector compressors: Report for oil and natural gas sector compressors review panel. Technical report, U.S. Environmental Protection Agency.

[Vaughn et al., 2020] Vaughn, T. L., Mitchell, A. L., Tkacik, D. S., Roscioli, J. R., Herndon, S. C., Yacovitch, T. I., Floerchinger, C., Williams, L. L., Zimmerle, D. J., and Marchese, A. J. (2020). Methane exhaust measurements at gathering compressor stations in the United States. Environmental Science & Technology, 54(11):6637–6647.

[Zavala-Araiza et al., 2017] Zavala-Araiza, D., Alvarez, R. A., Lyon, D. R., Allen, D. T., Marchese, A. J., Zimmerle, D. J., and Hamburg, S. P. (2017). Super-emitters in natural gas infrastructure are caused by abnormal process conditions. Nature Communications, 8:14012.

[Zavala-Araiza et al., 2015] Zavala-Araiza, D., Lyon, D. R., Alvarez, R. A., Davis, K. J., Harriss, R., Herndon, S. C., Karion, A., Kort, E. A., Lamb, B. K., Lan, X., Marchese, A. J., Pacala, S. W., Robinson, A. L., Shepson, P. B., Sweeney, C., Talbot, R., Townsend-Small, A., Yacovitch, T. I., Zimmerle, D. J., and Hamburg, S. P. (2015). Reconciling divergent estimates of oil and gas methane emissions. Proceedings of the National Academy of Sciences, 112(51):15597–15602.

[Zimmerle et al., 2019] Zimmerle, D., Bennett, K., Vaughn, T., Luck, B., Lauderdale, T., Keen, K., Harrison, M., Marchese, A., Williams, L., and Allen, D. (2019). Characterization of methane emissions from gathering compressor stations: Final report.

[Zimmerle et al., 2020] Zimmerle, D. J., Vaughn, T. L., Bell, C. S., Bennett, K. A., Deshmukh, P. J., Thoma, E. D., and Marchese, A. J. (2020). Methane emissions from gathering compressor stations in the United States. Environmental Science & Technology, 54(10):6448–6457.

[Zimmerle et al., 2015] Zimmerle, D. J., Williams, L. L., Vaughn, T. L., Quinn, C., Subramanian, R., Duggan, G. P., Willson, B., Opsomer, J. D., Marchese, A. J., Martinez, D. M., and Robinson, A. L. (2015). Methane Emissions from the Natural Gas Transmission and Storage System in the United States. Environmental Science & Technology, 49(15):9374–9383.

A SUPPLEMENTARY INFORMATION

A.1 Sensitivity to the HP stratification boundary

The 1000 HP boundary used to stratify the fractional loss distributions in the main text is an arbitrary cutoff to categorize the distinct engine sizes typically used in production and midstream applications. To confirm that the observed size effect is not an artifact of this choice, the class medians, means, and below/above-cutoff ratios were recomputed for both emission sources as the stratification boundary was varied from 750 to 1500 HP (Table 3). Across the 750–1250 HP range the direction and approximate magnitude of the size effect are preserved for both rod packing and blowdown. At a 1500 HP cutoff the smaller class absorbs the majority of units, so the contrast no longer isolates small compressors and the ratio compresses, as expected.

Table 3: Sensitivity of the size effect to the HP stratification boundary. Median and ratio of points above/below the cutoff are recomputed for rod packing (OP) and blowdown fractional loss as the cutoff is varied from 750 to 1500 HP. The direction and approximate magnitude of the size effect are preserved across the 750–1250 HP range for both sources. At a 1500 HP cutoff the smaller class dictates the majority of units (267 of 359 for rod packing, 67 of 88 for blowdown), so the contrast no longer isolates small compressors and the ratio compresses.

Source	**Cutoff (HP)**	$n_<$	$n_\geq$	**Median**$_<$	**Median**$_\geq$	**Median ratio**	**Mean ratio**
Rod Packing (OP)	750	29	330	2.54×10^{-5}	4.83×10^{-6}	5.2	8.3
Rod Packing (OP)	850	35	324	1.77×10^{-5}	4.85×10^{-6}	3.6	7.8
Rod Packing (OP)	1000	35	324	1.77×10^{-5}	4.85×10^{-6}	3.6	7.8
Rod Packing (OP)	1150	37	322	1.77×10^{-5}	4.85×10^{-6}	3.6	7.5
Rod Packing (OP)	1250	45	314	3.60×10^{-5}	4.76×10^{-6}	7.6	8.9
Rod Packing (OP)	1500	267	92	5.48×10^{-6}	3.00×10^{-6}	1.8	3.9
Blowdown	750	31	57	2.29×10^{-5}	3.76×10^{-7}	60.9	4.2
Blowdown	850	33	55	2.16×10^{-5}	3.76×10^{-7}	57.5	3.9
Blowdown	1000	33	55	2.16×10^{-5}	3.76×10^{-7}	57.5	3.9
Blowdown	1150	34	54	2.10×10^{-5}	3.54×10^{-7}	59.2	3.7
Blowdown	1250	36	52	2.10×10^{-5}	3.30×10^{-7}	63.5	4.1
Blowdown	1500	67	21	3.06×10^{-6}	5.84×10^{-8}	52.5	47.6

A.2 Gas composition for enthalpy evaluation

The specific enthalpy change Δh used to estimate throughput (Equation 3) was evaluated for the representative associated gas composition given in Table 4. The composition corresponds to the vapor stream compressed from the Stage 2 separator to pipeline pressure, and the same value is applied across all COBE facilities as described in Section 2.2.

Table 4: Composition of the representative Stage 2 associated gas used to evaluate the specific enthalpy change Δh for throughput estimation. Values are mole percentages of the vapor stream compressed from the Stage 2 separator (suction conditions 74.65 psia and 110 °F) to pipeline pressure. Evaluated with the GERG-2008 equation of state via REFPROP v10 [Kunz and Wagner, 2012, Lemmon et al., 2018], this composition and pressure boundary give $\Delta h = 14.74$ kJ/scf. Pseudocomponents 1 and 2 are lumped heavier fractions carried through from the flash model.

Component	**Composition (mol %)**
Nitrogen (N_2)	2.304
Carbon dioxide (CO_2)	2.544
Hydrogen sulfide (H_2S)	0.023
Methane (C_1)	60.871
Ethane (C_2)	17.319
Propane (C_3)	9.448
Isobutane (i-C_4)	1.377
n-Butane (n-C_4)	3.191
Isopentane (i-C_5)	0.700
n-Pentane (n-C_5)	0.655
Hexane (C_6)	0.652
Pseudocomponent 1	0.917
Pseudocomponent 2	0.0001
Total	100.00

A.3 Blowdown vent fractional loss envelope

The main text presents the blowdown vent fractional loss distribution as a cumulative distribution function stratified by HP class (Figure 5). Figure 7 presents the same data as a fractional loss versus rated power envelope, constructed with an independent log-log fit to the GEF blowdown measurements in the same manner as the rod packing seal condition envelope (Figure 6). The percentile bands describe the expected range of blowdown fractional loss as a function of compressor size.

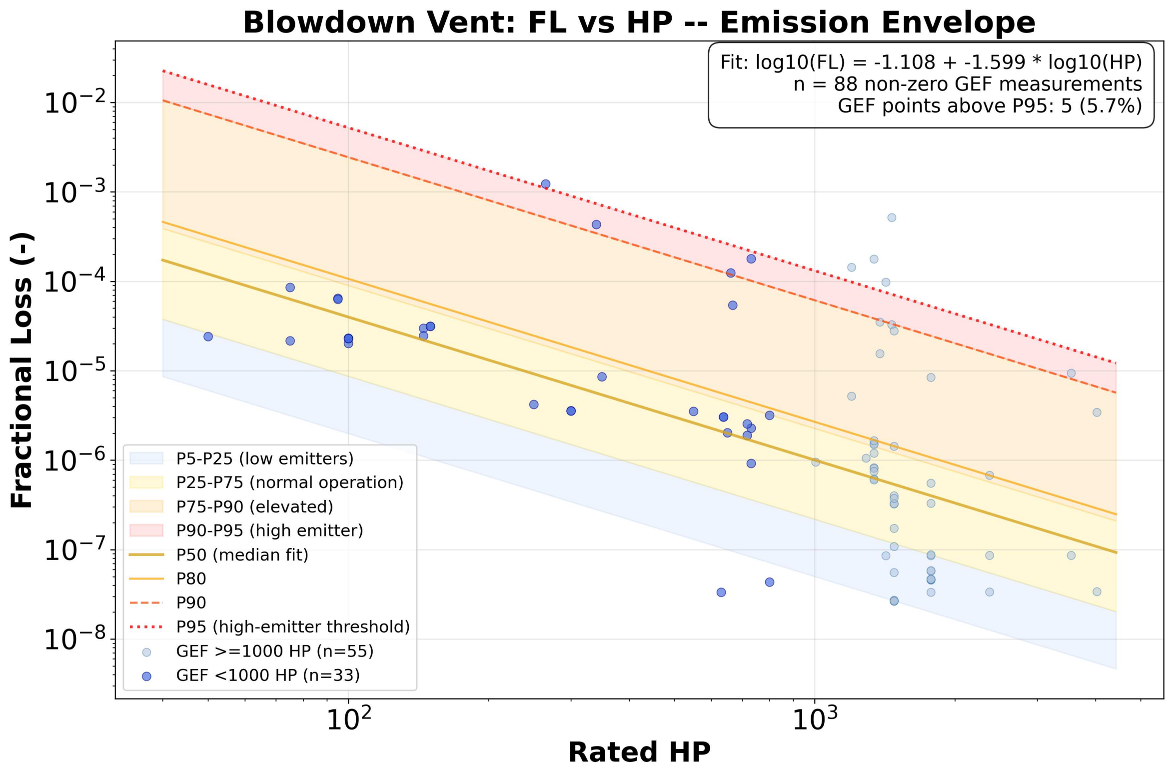

Figure 7: Blowdown vent fractional loss versus compressor rated power, with percentile bands from an independent log-log linear fit to the GEF blowdown measurements. Bands denote seal-analogous condition categories from low emitters (P5–P25) through elevated emission (P75–P90) to the high-emitter threshold (P95). GEF measurements are stratified by HP class.

A.4 Distribution of throughput per unit rated power

Throughput estimation from rated power (Equation 3) assumes a consistent relationship between a compressor's rated power and the gas volume it processes. Figure 8 shows the distribution of the throughput-to-rated-power ratio across the GEF facilities, stratified by HP class. The ratio varies widely within each class, with coefficients of variation of 84% below 1000 HP and 134% at or above 1000 HP, indicating that throughput per unit rated power is not fixed across the fleet. This spread is consistent with the throughput uncertainty discussed in Section 3.4 and reinforces that the enthalpy-based throughput estimate is an approximation applied where directly reported throughput is unavailable.

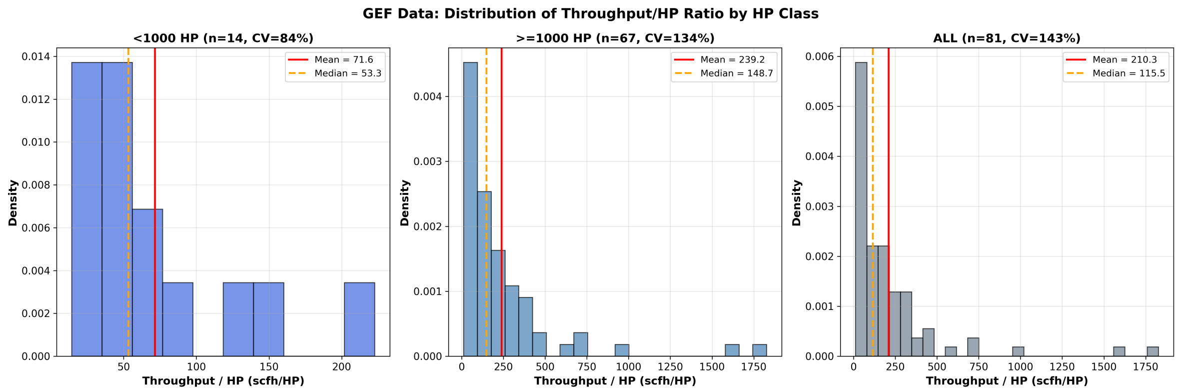

Figure 8: Distribution of the throughput-to-rated-power ratio (scfh/HP) across GEF facilities, stratified by compressor HP class. Vertical lines mark the class mean (solid) and median (dashed). The wide spread within each class, quantified by coefficients of variation of 84% (<1000 HP) and 134% (≥1000 HP), reflects facility-to-facility variability in gas throughput relative to rated power.

A.5 Per-facility emission and fractional loss data

Tables 5 and 6 report the per-facility fractional loss and emission rate data underlying the distributions in Section 3.1, for rod packing (OP) and blowdown vents respectively. Each facility contributes one or more measurements, and the median fractional loss and median emission rate across those measurements are reported alongside the measurement count. Fractional loss is the ratio of emission rate to throughput (Equation 1).

Table 5: Per-facility rod packing (OP) data from the GEF study: rated power, facility throughput, measurement count, and median fractional loss and emission rate across each facility's measurements. Eighty-one facilities contribute the 359 rod packing OP measurements.

Facility ID	Rated HP	Throughput (scfh)	n	Median FL	Median ER (scfh)
17	1480	329,167	2	2.67×10^{-4}	87.87
40	1480	337,500	3	6.56×10^{-5}	22.13
55	1480	750,000	14	9.91×10^{-6}	7.43
66	1480	4,666,667	53	3.68×10^{-7}	1.72
94	340	50,000	1	7.23×10^{-4}	36.16
136	580	129,167	1	8.02×10^{-5}	10.36
216	1340	208,333	2	9.24×10^{-5}	19.25
235	2370	1,750,000	2	7.99×10^{-6}	13.98
251	1380	854,167	2	2.43×10^{-4}	207.34
252	1775	2,416,667	4	5.89×10^{-8}	0.14
333	1775	2,375,000	4	4.62×10^{-8}	0.11
430	1340	208,333	5	2.94×10^{-5}	6.12
441	2370	4,250,000	12	1.15×10^{-7}	0.49
492	1340	312,500	9	7.13×10^{-7}	0.22
509	1035	175,000	1	1.35×10^{-4}	23.59
512	1775	845,833	3	2.64×10^{-5}	22.34
570	1765	525,083	2	4.22×10^{-5}	22.17
604	1380	420,833	1	7.91×10^{-4}	332.79
634	1480	600,000	7	5.12×10^{-5}	30.73
640	730	70,833	2	2.28×10^{-6}	0.16
660	1340	816,667	1	1.63×10^{-5}	13.32
744	1340	370,833	3	3.28×10^{-5}	12.17
765	1289	291,667	7	3.22×10^{-5}	9.39

Table 5 – continued from previous page

Facility ID	Rated HP	Throughput (scfh)	n	Median FL	Median ER (scfh)
790	1775	990,000	2	6.07×10^{-5}	60.08
791	1340	112,500	7	4.07×10^{-5}	4.58
818	1480	2,000,000	9	1.06×10^{-6}	2.11
952	1340	333,333	2	5.93×10^{-5}	19.78
1011	686	31,250	3	1.28×10^{-4}	4.00
1080	1380	395,833	1	5.07×10^{-5}	20.07
1120	1350	179,167	5	1.48×10^{-5}	2.65
1126	1775	616,667	1	3.63×10^{-7}	0.22
1141	1289	160,417	3	7.30×10^{-5}	11.71
1165	467	500,000	8	2.68×10^{-5}	13.42
1167	1420	70,833	1	5.71×10^{-6}	0.40
1259	1340	6,777,833	2	1.54×10^{-5}	104.42
1291	1340	125,000	1	1.21×10^{-6}	0.15
1292	1380	4,975,000	32	4.79×10^{-6}	23.84
1418	1400	1,208,333	12	9.89×10^{-6}	11.95
1451	1775	366,667	1	2.54×10^{-5}	9.31
1461	4025	4,166,667	8	1.39×10^{-7}	0.58
1496	1775	1,216,667	4	3.33×10^{-5}	40.52
1536	203	37,500	2	3.35×10^{-6}	0.13
1564	1340	1,384,417	5	1.70×10^{-5}	23.52
1592	800	69,500	2	1.50×10^{-6}	0.10
1618	1775	1,325,000	2	1.34×10^{-5}	17.70
1633	1380	583,333	1	1.93×10^{-5}	11.23
1644	1380	325,000	3	4.24×10^{-5}	13.78
1652	550	41,667	1	3.55×10^{-6}	0.15
1661	1340	64,583	4	9.45×10^{-4}	61.04
1681	1340	579,167	1	2.51×10^{-5}	14.54
1779	250	25,708	2	2.23×10^{-3}	57.35
1785	1775	3,854,167	10	9.57×10^{-7}	3.69
1825	2370	1,666,667	1	8.52×10^{-8}	0.14
1830	580	16,667	2	5.61×10^{-4}	9.35
1873	2370	1,625,000	1	8.72×10^{-8}	0.14
1945	1775	204,167	1	1.48×10^{-4}	30.14
2048	1380	2,208,333	1	2.66×10^{-5}	58.70
2057	717	82,958	2	1.91×10^{-6}	0.16
2064	3665	450,000	2	1.77×10^{-5}	7.97
2073	3550	433,333	6	6.51×10^{-5}	28.20
2149	1340	289,375	1	5.06×10^{-5}	14.63
2291	1232	75,000	5	3.60×10^{-4}	26.97
2307	800	44,583	2	2.02×10^{-4}	8.99
2416	1380	495,833	2	8.40×10^{-6}	4.16
2451	1340	215,917	2	5.55×10^{-7}	0.12
2469	650	53,708	5	1.04×10^{-4}	5.59
2491	1480	447,750	9	8.29×10^{-6}	3.71
2516	1340	575,000	10	3.18×10^{-6}	1.83
2557	1775	1,312,500	5	1.18×10^{-5}	15.45
2588	3300	950,000	9	6.09×10^{-6}	5.79
2610	1775	270,833	1	7.47×10^{-5}	20.24
2643	2370	2,456,583	4	4.12×10^{-5}	101.22
2691	3300	129,167	1	8.39×10^{-4}	108.34
2783	830	45,833	1	5.14×10^{-4}	23.57
2785	1420	229,167	1	1.02×10^{-4}	23.43

Table 5 – continued from previous page

Facility ID	Rated HP	Throughput (scfh)	n	Median FL	Median ER (scfh)
2827	1340	302,292	2	2.81×10^{-5}	8.51
2833	1775	608,333	1	2.72×10^{-5}	16.56
2856	1775	1,766,667	1	1.99×10^{-5}	35.16
2874	1150	750,000	3	3.33×10^{-5}	24.95
2963	1004	116,000	1	9.40×10^{-7}	0.11
2964	1340	294,125	1	4.95×10^{-5}	14.56

Table 6: Per-facility blowdown vent data from the GEF study: rated power, facility throughput, measurement count, and median fractional loss and emission rate across each facility's measurements. Fifty facilities contribute the 88 blowdown measurements.

Facility ID	Rated HP	Throughput (scfh)	n	Median FL	Median ER (scfh)
17	1480	329,167	2	3.26×10^{-7}	0.11
40	1480	337,500	1	4.03×10^{-7}	0.14
55	1480	750,000	1	1.74×10^{-7}	0.13
66	1480	4,666,667	8	2.70×10^{-8}	0.13
83	50	5,208	1	2.43×10^{-5}	0.13
85	95	1,917	1	6.45×10^{-5}	0.12
94	340	50,000	1	4.35×10^{-4}	21.73
119	95	2,000	1	6.31×10^{-5}	0.13
165	75	5,833	1	2.16×10^{-5}	0.13
216	1340	208,333	2	8.18×10^{-7}	0.17
244	145	4,208	1	2.99×10^{-5}	0.13
247	667	45,833	1	5.40×10^{-5}	2.48
252	1775	2,416,667	2	5.80×10^{-8}	0.14
315	800	3,945,833	1	4.36×10^{-8}	0.17
333	1775	2,375,000	6	4.64×10^{-8}	0.11
556	1340	162,500	1	7.52×10^{-7}	0.12
640	730	70,833	2	9.04×10^{-5}	6.41
772	1200	718,750	2	7.42×10^{-5}	53.36
818	1480	2,000,000	1	5.58×10^{-8}	0.11
1141	1289	160,417	1	1.06×10^{-6}	0.17
1171	265	17,958	1	1.23×10^{-3}	22.02
1291	1340	125,000	2	8.97×10^{-5}	11.21
1437	100	6,250	1	2.03×10^{-5}	0.13
1461	4025	4,166,667	6	3.38×10^{-8}	0.14
1633	1380	583,333	1	1.55×10^{-5}	9.05
1643	145	6,250	1	2.47×10^{-5}	0.15
1652	550	41,667	2	6.40×10^{-5}	2.66
1660	1463	279,167	2	2.75×10^{-4}	76.67
1738	1775	500,000	3	5.53×10^{-7}	0.28
1756	1340	120,000	2	1.52×10^{-6}	0.18
1779	250	25,708	1	4.22×10^{-6}	0.11
1825	1775	1,666,667	1	8.61×10^{-8}	0.14
1846	350	14,583	1	8.57×10^{-6}	0.12
1873	3550	1,625,000	4	8.74×10^{-8}	0.14
2057	717	82,958	2	2.23×10^{-6}	0.18
2188	1340	75,000	1	1.66×10^{-6}	0.12
2214	1340	262,500	2	6.13×10^{-7}	0.16
2285	75	1,458	1	8.57×10^{-5}	0.13
2307	800	44,583	1	3.18×10^{-6}	0.14

Table 6 – continued from previous page

Facility ID	**Rated HP**	**Throughput (scfh)**	n	**Median FL**	**Median ER (scfh)**
2407	100	5,417	2	2.31×10^{-5}	0.13
2420	150	3,958	2	3.15×10^{-5}	0.12
2469	650	53,708	1	2.03×10^{-6}	0.11
2491	1480	447,750	1	2.80×10^{-5}	12.54
2586	100	5,417	1	2.30×10^{-5}	0.12
2607	637	70,833	2	3.05×10^{-6}	0.22
2643	2370	2,456,583	1	6.77×10^{-7}	1.66
2785	1420	229,167	1	9.82×10^{-5}	22.51
2927	1380	500,000	1	3.50×10^{-5}	17.52
2956	300	35,417	2	3.56×10^{-6}	0.13
2963	1004	116,000	2	9.38×10^{-7}	0.11